

Be abundances in cool main-sequence stars with exoplanets¹

E. Delgado Mena^{1,2}, G. Israelian^{1,2}, J. I. González Hernández^{1,2}, N. C. Santos^{3,4} and R. Rebolo^{1,2,5}

ABSTRACT

We present new UVES spectra of a sample of 15 cool unevolved stars with and without detected planetary companions. Together with previous determinations, we study Be depletion and possible differences in Be abundances between both groups of stars. We obtain a final sample of 89 and 40 stars with and without planets, respectively, which covers a wide range of effective temperatures, from 4700 K to 6400 K, and includes several cool dwarf stars for the first time.

We determine Be abundances for these stars and find that for most of them (the coolest ones) the BeII resonance lines are often undetectable, implying significant Be depletion. While for hot stars Be abundances are approximately constant, with a slight fall as T_{eff} decreases and the Li-Be gap around 6300 K, we find a steep drop of Be content as T_{eff} decreases for $T_{\text{eff}} < 5500$ K, confirming the results of previous papers. Therefore, for these stars there is an unknown mechanism destroying Be that is not reflected in current models of Be depletion.

Moreover, this strong Be depletion in cool objects takes place for all the stars regardless of the presence of planets, thus, the effect of extra Li depletion in solar-type stars with planets when compared with stars without detected planets does not seem to be present for Be, although the number of stars at those temperatures is still small to reach a final conclusion.

Subject headings: stars: abundances - stars: fundamental parameters - planetary systems - planets and satellites: formation - stars: atmospheres

1. Introduction

Light elements are important tracers of stellar internal mixing and rotation. Since they are burned at relatively low temperatures they constrain how the material inside stars is mixed with the hotter interior. Rotation and angular momentum loss are among the leading processes to explain the mixing that leads to depletion of light

elements in solar-type stars (e.g. Stephens et al. 1997; Bouvier 2008) although gravitational waves may also affect the abundances of those elements (Montalbán & Schatzman 2000). However, available models for evolution of Be (considering rotation) do not predict a significant depletion of Be during the main sequence for stars with $6000 \text{ K} > T_{\text{eff}} > 4000 \text{ K}$ (Pinsonneault et al. 1990). On the other hand, models which take into account gravitational waves predict significant Be depletion only for stars cooler than 4500 K (Montalbán & Schatzman 2000).

In a recent work, Israelian et al. (2009) confirmed that Li was severely depleted in solar-type stars (with T_{eff} between 5600 K and 5850 K) with planets when compared with similar stars without detected planets although this result is controversial (Baumann et al. 2010; Sousa et al. 2010); for a complete discussion see Delgado Mena et al.

¹Instituto de Astrofísica de Canarias, 38200 La Laguna, Tenerife, Spain: edm@iac.es

²Departamento de Astrofísica, Universidad de La Laguna, 38206 La Laguna, Tenerife, Spain

³Centro de Astrofísica, Universidade do Porto, Rua das Estrelas, 4150-762 Porto, Portugal

⁴Departamento de Física e Astronomia, Faculdade de Ciências, Universidade do Porto, Portugal

⁵Consejo Superior de Investigaciones Científicas, Spain

¹Based on observations made with UVES at VLT Kueyen 8.2 m telescope at the European Southern Observatory (Cerro Paranal, Chile) in program 86.D-0082A

(2011). This difference in Li abundance seems to be related to the different rotational history of both groups of stars due to the presence of protoplanetary disks (e.g. Bouvier 2008). However, beryllium needs a greater temperature to be burned so we would expect to see the onset of this effect in cooler stars where convective envelopes are deep enough to reach those higher temperatures.

In a previous paper, Delgado Mena et al. (2011) found two cool planet host stars with an extra depletion of Be when compared with analog stars without detected planets. This encourages us to try to investigate this process in cool stars. In this work we continue that analysis by extending the sample with 15 new cool stars. We refer the reader to that paper for further information and a more extensive introduction.

2. Observations and spectral synthesis

In this study we obtained high resolution spectra for 15 new stars with magnitudes V between 6 and 10 using the UVES spectrograph at the 8.2-m Kueyen VLT (UT2) telescope (run ID 86.D-0082A) between October 2010 and March 2011. The dichroic mirror was used to obtain also red spectra and the slit width was 0.5 arcsec. These new spectra have a spectral resolution $R \sim 70000$ and S/N ratios between 100 and 200. All the data were reduced with the pipeline of *UVES/VLT*. Standard background correction, flat-field and extraction procedures were used. The wavelength calibration was made using a ThAr lamp spectrum taken during the same night. Finally we manually normalized the continuum by dividing the spectra by a spline function with three pieces (and the parameter *low - reject* set to 1) in the whole blue region (3040Å-3800Å). This normalization does not present any bias for stars with and without planets. When plotting together observed spectra of stars with and without planets we only had to multiply the flux of comparison stars by 0.9-1.1 in order to make them match up. We note that in our previous works we have analyzed high metallicity (up to 0.4) solar type stars with T_{eff} down to 5300 K for which we could make a good normalization. The main problem is the normal-

ization of spectra of stars with T_{eff} less than ~ 5300 K. These stars could have spots and inhomogeneous atmospheres that make the spectral synthesis more difficult.

The uniform stellar atmospheric parameters were taken from Sousa et al. (2008) with typical errors of 25 K for T_{eff} , 0.04 dex for $\log g$, 0.03 km s $^{-1}$ for ξ_t and 0.02 dex for metallicity. We refer to that work for further details in these parameters and their uncertainties.

Be abundances were derived by fitting the spectral region around the Be II line at 3131.06 Å and then using the Be II line 3130.42 Å to check the consistency of the fit. We used an empirical line list from García López et al. (1995) tuned to reproduce the solar spectrum (see Table 1). These synthetic spectra were convolved with a rotational profile. We made a standard LTE analysis with the revised version of the spectral synthesis code MOOG2002 (Snedden 1973) and a grid of Kurucz ATLAS9 atmospheres with overshooting (Kurucz et al. 1993). Examples of synthetic spectra and the parameters used in the synthesis are shown in Figure 1.

The final sample is composed of 70 and 30 stars with and without planets, respectively, from Santos et al. (2002, 2004a,c); Gálvez-Ortiz et al. (2011), 14 stars with planets from Delgado Mena et al. (2011) and 5 and 10 stars with and without detected planets, respectively, from this work. This gives a total sample of 89 stars with planets and 40 comparison sample stars. All Be abundances for these 89+40 stars were analyzed by our team using the same methodology, making this a very uniform sample.

TABLE 1
KURUCZ LINE LIST TUNED TO REPRODUCE SOLAR SPECTRUM.

$\lambda(\text{\AA})$	Atomic number	χ (eV)	gf	$\lambda(\text{\AA})$	Atomic number	χ (eV)	gf
3127.968	108.0	1.670	0.461E-03	3130.420	4.1	0.000	0.670E+00
3128.060	108.0	0.541	0.376E-02	3130.433	108.0	1.756	0.428E-02
3128.101	108.0	0.210	0.131E-02	3130.439	25.0	3.772	0.303E-02
3128.154	108.0	1.599	0.101E-03	3130.473	108.0	1.609	0.603E-03
3128.166	25.1	6.914	0.190E-02	3130.476	26.0	3.573	0.092E-02
3128.172	25.0	7.822	0.228E-03	3130.549	25.1	6.494	0.714E-01
3128.237	108.0	0.442	0.475E-03	3130.562	26.1	3.768	0.612E-05
3128.269	21.1	7.424	0.675E+00	3130.569	24.1	5.330	0.349E-02
3128.286	108.0	0.210	0.104E-01	3130.570	108.0	0.683	0.298E-01
3128.289	108.0	0.442	0.728E-03	3130.575	23.0	1.218	0.543E-03
3128.304	23.1	2.376	0.134E+00	3130.577	73.0	1.394	0.117E+01
3128.307	607.0	0.513	0.288E-04	3130.585	24.0	3.556	0.108E-01
3128.308	607.0	0.513	0.249E-04	3130.637	25.0	4.268	0.982E-01
3128.356	108.0	1.714	0.245E-02	3130.648	106.0	0.034	0.02009
3128.377	108.0	1.714	0.333E-03	3130.780	41.1	0.439	0.257E+01
3128.393	77.0	1.728	0.110E+00	3130.791	45.0	0.431	0.776E-02
3128.394	106.0	0.558	0.731E-01	3130.803	22.1	0.012	0.589E-01
3128.394	106.0	0.558	0.800E-01	3130.813	64.1	1.157	0.826E+00
3128.406	66.1	1.314	0.226E+01	3130.842	23.0	1.955	0.119E-02
3128.488	22.1	7.867	0.151E+01	3130.851	26.2	11.595	0.527E-03
3128.495	22.1	2.590	0.908E-05	3130.871	58.1	1.090	0.957E-01
3128.518	108.0	0.786	0.817E-02	3130.905	26.1	7.487	0.100E-02
3128.524	108.0	0.102	0.500E-03	3130.928	106.0	0.002	0.231E-03
3128.546	24.1	4.757	0.859E-02	3130.928	108.0	1.907	0.946E-03
3128.568	64.1	1.134	0.787E+00	3130.933	108.0	0.683	0.294E-03
3128.617	22.0	5.959	0.658E-03	3130.997	108.0	1.569	0.137E-03
3128.618	22.0	1.067	0.883E-03	3131.015	25.1	6.112	0.607E-01
3128.626	22.0	6.065	0.643E+00	3131.037	25.0	3.773	0.596E+00
3128.641	25.1	6.672	0.714E-01	3131.059	25.1	6.672	0.191E-02
3128.648	26.1	12.966	0.855E-02	3131.065	4.1	0.000	0.338E+00
3128.653	607.0	0.510	0.249E-04	3131.070	90.1	0.000	0.276E-01
3128.653	607.0	0.510	0.210E-04	3131.102	26.1	9.688	0.695E-01
3128.692	24.1	2.434	0.479E+00	3131.109	40.0	0.520	0.398E+00
3128.692	29.0	4.974	0.195E+00	3131.115	26.0	3.047	0.194E-05
3128.694	23.1	2.372	0.430E+00	3131.116	76.0	1.841	0.112E+01
3128.728	28.0	1.951	0.512E-04	3131.143	22.0	0.836	0.279E-05
3128.737	39.1	3.376	0.646E+01	3131.194	42.0	2.499	0.441E-01
3128.763	72.0	0.000	0.170E-01	3131.212	24.0	3.113	0.604E+00
3128.776	23.0	1.804	0.126E-01	3131.243	26.0	2.176	1.726E-04
3128.782	108.0	0.897	0.102E-01	3131.255	69.1	0.000	0.240E+00
3128.854	23.0	1.712	0.205E-03	3131.326	27.1	2.204	0.817E-04

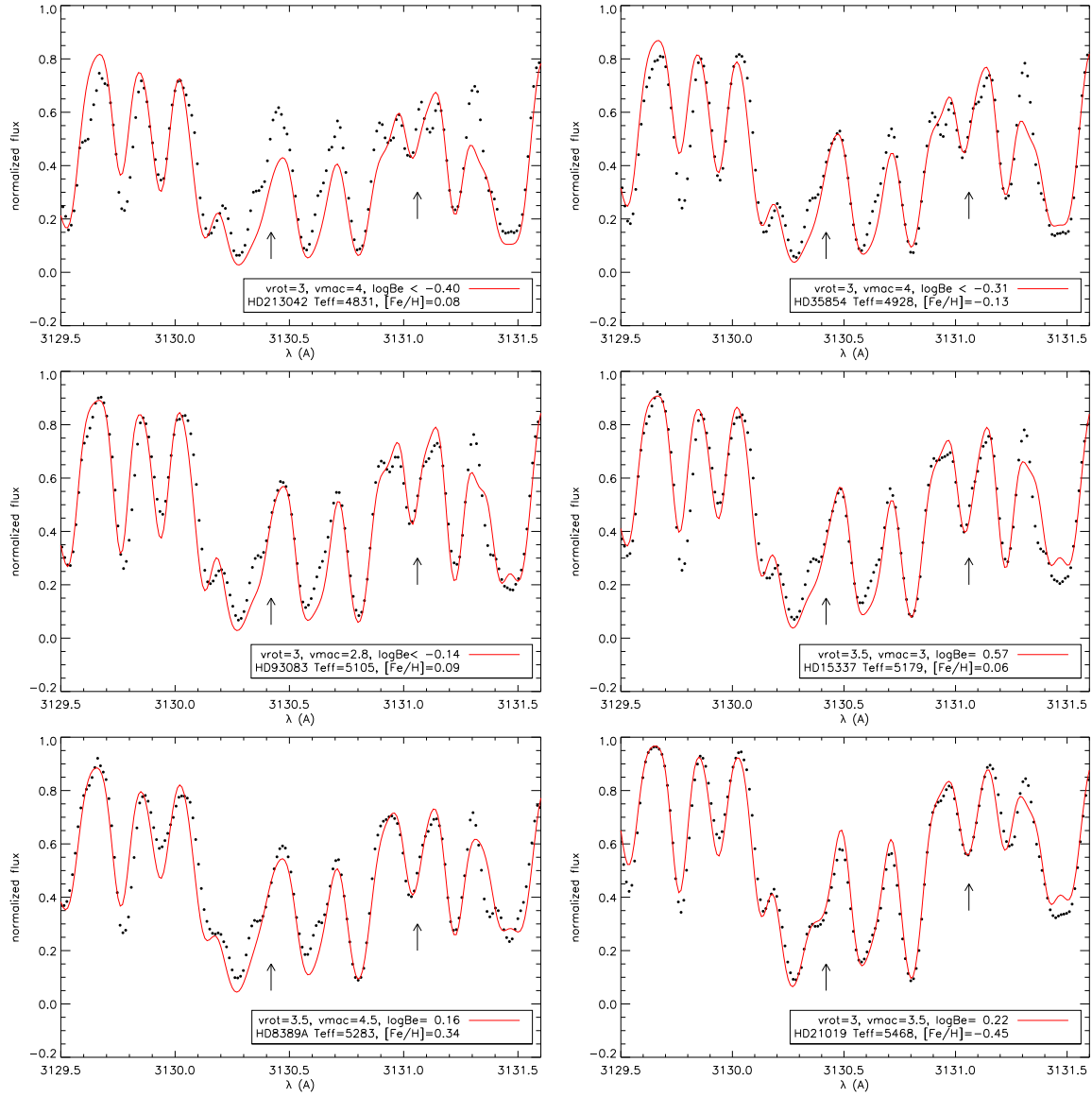


Fig. 1.— Synthetic spectra (red lines) and observed spectra (dots) for the planet host star HD 93083 and the stars without detected planets HD 213042, HD 35854, HD 15337, HD 8389A and HD 21019. The position of Be lines are indicated by the arrows.

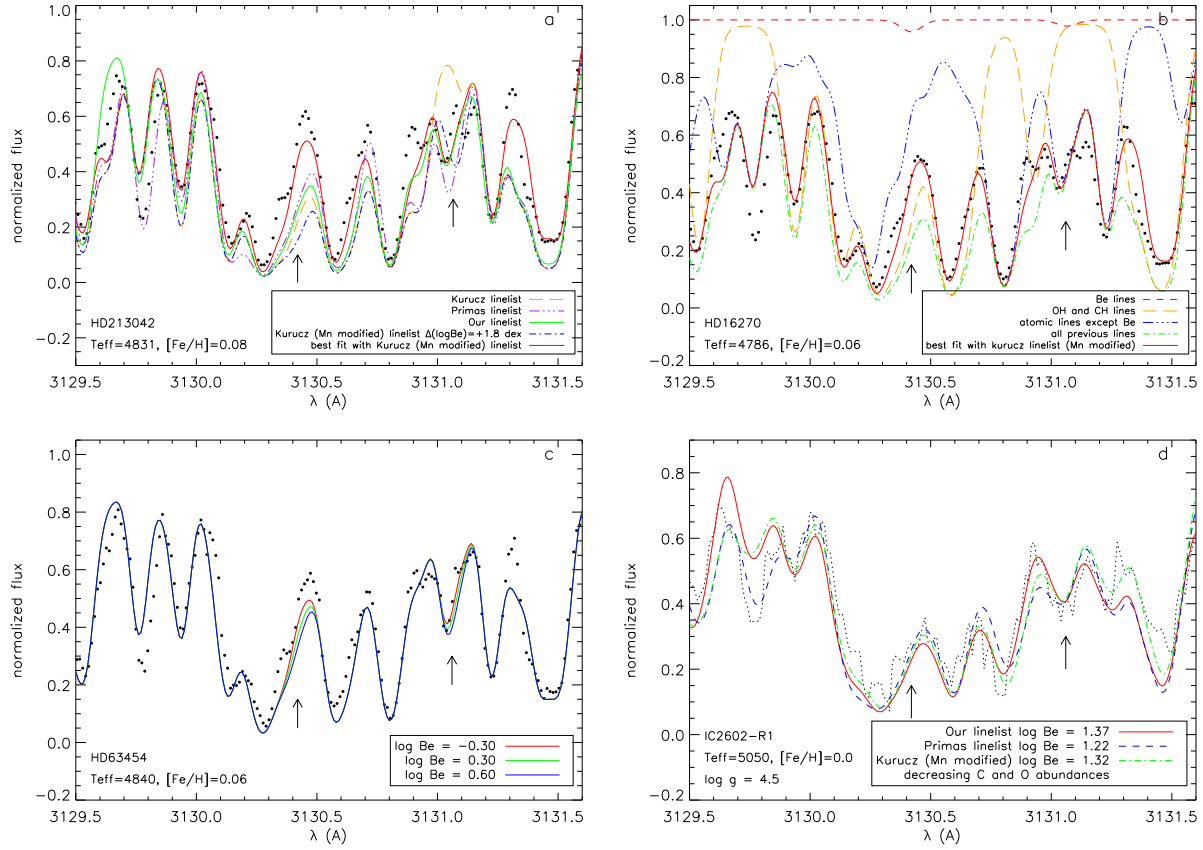


Fig. 2.— Panel a: Spectral synthesis of HD 213042 using different line lists. Panel b: Spectral synthesis of HD 16270 showing the contributions of atomic, molecular and Be lines. Panel c: Spectral synthesis of HD 63454 with solar line list and different values of Be abundance. Panel d: Spectral synthesis of the star R1 in the young cluster IC 2602 using different line lists.

TABLE 1—*Continued*

$\lambda(\text{\AA})$	Atomic number	χ (eV)	gf	$\lambda(\text{\AA})$	Atomic number	χ (eV)	gf
3128.898	26.0	1.557	0.223E-02	3131.329	108.0	1.942	0.160E-01
3128.938	108.0	1.939	0.254E-03	3131.338	25.0	4.679	0.117E-01
3128.949	75.0	2.061	0.166E+01	3131.339	21.1	7.381	0.372E-02
3128.954	25.0	2.920	0.447E-04	3131.366	108.0	1.942	0.250E-03
3128.975	108.0	1.939	0.169E-01	3131.384	108.0	1.680	0.604E-03
3129.001	607.0	0.508	0.210E-04	3131.394	108.0	1.680	0.511E-03
3129.005	27.0	0.514	0.117E-02	3131.395	26.1	3.815	0.221E-03
3129.009	26.1	3.968	0.202E-02	3131.423	108.0	0.960	0.789E-02
3129.009	26.1	12.966	0.340E-02	3131.458	25.1	4.340	0.294E-04
3129.013	24.1	12.978	0.873E+00	3131.459	26.0	6.427	0.234E-04
3129.017	107.0	0.740	0.202E-04	3131.486	28.1	12.409	0.755E-02
3129.038	26.2	10.311	0.229E-03	3131.502	108.0	0.494	0.185E-02
3129.070	22.0	6.079	0.971E+00	3131.525	28.0	7.152	0.126E-02
3129.095	108.0	0.897	0.574E-03	3131.533	24.1	4.168	0.782E-02
3129.110	20.0	4.625	0.185E-02	3131.545	80.0	4.887	0.912E+00
3129.138	107.0	0.740	0.211E-04	3131.548	24.1	4.178	0.350E-01
3129.144	24.1	7.332	0.498E-01	3131.583	25.1	6.495	0.124E-01
3129.153	40.1	0.527	0.479E+00	3131.656	107.0	0.787	0.140E-03
3129.182	26.0	6.411	0.349E-04	3131.687	108.0	1.736	0.193E-01
3129.183	22.0	1.046	0.160E-03	3131.702	28.0	7.264	0.247E-01
3129.209	107.0	0.740	0.223E-04	3131.711	108.0	1.736	0.319E-03
3129.210	24.0	3.556	0.490E-01	3131.724	26.1	4.081	0.486E-02
3129.228	76.0	2.191	0.537E+00	3131.754	108.0	0.960	0.550E-03
3129.300	28.0	0.275	0.625E-02	3131.812	72.0	1.306	0.263E+01
3129.305	66.0	0.000	0.135E-01	3131.825	27.0	1.740	0.161E-01
3129.333	26.0	1.485	0.114E-01	3131.838	80.0	4.887	0.912E+00
3129.348	25.0	3.379	0.490E-04	3131.935	107.0	0.787	0.148E-03
3129.348	25.0	3.379	0.195E-03	3132.053	24.1	2.483	0.120E+01
3129.376	11.1	32.944	0.102E+01	3132.062	22.0	5.975	0.530E-03
3129.389	23.0	2.115	0.979E-03	3132.063	40.0	0.543	0.105E+01
3129.454	8.1	25.640	0.290E+00	3132.109	24.1	4.775	0.643E-04
3129.478	23.1	8.574	0.152E+00	3132.142	23.0	0.262	0.589E-05
3129.481	27.0	1.883	0.951E-02	3132.186	108.0	0.901	0.964E-02
3129.538	108.0	0.516	0.178E-02	3132.193	107.0	0.787	0.160E-03
3129.548	73.0	1.147	0.107E+00	3132.212	27.0	0.101	0.377E-01
3129.589	72.0	0.000	0.135E-01	3132.281	106.0	0.488	0.661E-01
3129.636	22.0	1.443	0.158E-02	3132.281	106.0	0.488	0.592E-01
3129.652	41.1	1.321	0.115E+00	3132.288	25.0	4.332	0.316E+00
3129.763	40.1	0.039	0.331E+00	3132.355	23.0	1.043	0.984E-04
3129.774	24.0	2.708	0.344E-02	3132.392	108.0	1.990	0.131E-03
3129.857	24.0	2.968	0.845E-02	3132.405	25.0	3.373	0.818E-02

3. Analysis

In general, Be abundances for stars cooler than 5200 K are probably not reliable since in this regime Be lines are barely sensitive to changes in the abundance. In Figure 1 we can observe that for the coolest stars the fits are not good. At those temperatures Mn I line at 3129.037 Å dominates the feature and the presence of Be is negligible (see also García López et al. 1995). We make several tests to try to improve those fits.

In Figure 2 we show several spectral syntheses. In panel *a* we have used different line lists for HD 213042. The orange dashed line is a fit made with original Kurucz line list². It is clear that the Mn-Be feature cannot be well reproduced with the original value of $\log gf$ for Mn line even if we increase Be abundance (light blue dashed-pointed line). Furthermore, the lambda of the whole feature do not match Be line, so this star do not present so much Be and another line is required to fit the observed spectrum. Primas et al. (1997) used an artificial Fe line at 3131.043 which in our case does not help to fit the spectrum (purple dashed-three pointed line) since this line gets stronger in metallic stars. Another option is to increase the gf of Mn line at 3131.037 Å. This was first proposed by García López et al. (1995) to reproduce solar spectrum and we also used this modified line in our previous works on Be. The green line represents a fit with Kurucz line list and this modified line. We note that for our syntheses we have used Mn measured abundances by Neves et al. (2009) with the same models. This fit is better but the feature is still stronger than observed in its red wing although the Be abundance used in the synthesis is negligible. The synthetic spectra of these cool stars present strong molecular lines. If we decrease O and C abundances (red line) we can get a better fit though this does not affect Be line at 3131.06 Å.

The different contributions of molecular and atomic lines is shown in panel *b* for star HD 16270. The Mn-Be feature is practically filled with atomic lines, that is, Mn line. Therefore we can put an upper limit in Be abundance since increasing Be abundance would result in a stronger line with a

core shifted towards higher λ which would not fit the observed spectrum. We can again get a better fit if we decrease O and C abundances (red line). However, as the stars get cooler we need to use lower C and O abundances, ~ -0.6 dex for O and ~ -0.9 dex for C in this star. This is not a realistic approach but fortunately C and O abundances hardly affect the Be feature.

In panel *c* we show three syntheses for HD 63454 with the solar line list derived by García López et al. (1995) and decreasing C and O abundances -0.3 and -0.2 dex respectively. The fits with $\log Be = 0.6$ and 0.3 dex presents a stronger line than observed, so we can adopt an upper limit of 0.0 dex for this star. Certainly, Be line is not very sensitive at these low temperatures and we think that we may be overestimating Be depletion. However, it is impossible to fit the spectra using high Be abundances so we can put an upper limit in Be content though we cannot calculate accurate abundances. Moreover, the sensitivity of Be line does not seem to be related to T_{eff} since some cool young objects present strong Be lines with abundances similar to solar (Smiljanic et al. 2011; Randich et al. 2007). This is the case of the star R1 in the young cluster IC 2602 of 46 Myr and solar metallicity. This star was observed by Smiljanic et al. (2011) who found $\log Be = 1.25$. We have analyzed this star using the same spectrum and three different line lists (see panel *d* of Figure 2): Primas et al. (1997) line list, used by these authors, gives $\log Be = 1.22$; our solar line list gives $\log Be = 1.37$ and Kurucz line list with Mn line modified and decreasing C and O abundances by 0.3 dex gives $\log Be = 1.32$, all of them in perfect agreement with the value previously found. Therefore, this test probably suggests that our line list does work for cool stars which present a measurable quantity of Be, and our fittings should be valid at least to put an upper limit in Be abundances.

4. Discussion

In this section we will discuss the different trends of Be abundances with the effective temperature, the metallicity and the oxygen abundance.

²http://kurucz.harvard.edu/line_lists.html

TABLE 1—*Continued*

$\lambda(\text{\AA})$	Atomic number	χ (eV)	gf	$\lambda(\text{\AA})$	Atomic number	χ (eV)	gf
3129.934	39.1	3.414	0.955E+01	3132.517	68.1	1.402	0.320E+01
3129.937	108.0	1.609	1.955E-02	3132.518	26.0	7.168	0.316E+00
3129.943	73.0	0.697	0.724E-01	3132.532	24.1	6.805	0.387E-03
3129.968	64.1	1.172	0.627E+00	3132.579	26.1	7.495	0.161E-02
3129.974	90.1	1.287	0.172E+00	3132.583	108.0	1.612	0.314E-01
3130.056	40.0	0.519	0.200E+00	3132.591	58.1	0.295	0.288E+00
3130.063	26.1	13.018	0.416E-02	3132.594	42.0	0.000	0.237E+01
3130.075	108.0	2.295	0.0029174	3132.596	23.1	2.900	0.859E-01
3130.126	108.0	0.842	0.794E-02	3132.631	607.0	0.510	0.210E-04
3130.145	108.0	1.987	0.0141579	3132.656	73.0	0.491	0.110E+00
3130.157	22.0	5.941	0.346E+00	3132.657	27.0	2.878	0.240E-04
3130.202	25.1	4.801	0.193E+00	3132.710	22.0	5.954	0.171E+00
3130.254	106.0	0.521	0.0660693	3132.725	25.1	6.177	0.215E-02
3130.257	23.1	0.348	0.513E+00	3132.788	25.0	4.268	0.316E+00
3130.281	108.0	0.250	0.134E-01	3132.794	8.2	36.895	0.933E+00
3130.290	106.0	0.521	0.0731139	3132.809	23.1	2.510	0.297E-01
3130.340	58.1	0.529	0.705E+00	3132.816	108.0	1.947	0.313E-03
3130.353	27.1	2.985	0.465E-03	3132.822	24.0	3.122	0.322E+00
3130.370	106.0	0.033	0.111E-01	3132.845	108.0	1.947	0.348E-02
3130.376	22.0	1.430	0.275E-01	3132.864	28.1	2.865	0.223E-03
3130.407	108.0	1.756	0.324E-03	3132.865	108.0	0.686	0.578E-03
3130.408	108.0	1.670	0.103E-03	3132.878	44.0	1.317	0.174E+00

*ine list used by García López et al. (1995) and in our previous works. The dissociation energy for OH, CH, NH and CN molecules is 4.39, 3.46, 3.47 and 7.65 eV respectively.

TABLE 2
STARS ANALYZED IN THIS WORK.

Star	T_{eff} [K]	$\log g$ [cm s ⁻²]	ξ_t [km s ⁻¹]	[Fe/H]	V	planet	Spectral type ^a	$\log \epsilon(\text{Be})$	$\log \epsilon(\text{Li})$
HD2638	5198	4.43	0.74	0.12	9.44	yes	G5	0.49	<0.16
HD8326	4971	4.48	0.81	0.02	8.70	no	K2V	j-0.16	<0.09
HD8389A	5283	4.37	1.06	0.34	7.84	no	K0VCN+2	0.16	<0.73
HD9796	5179	4.38	0.66	-0.25	8.81	no	K0V	0.27	<0.17
HD11964A ^b	5332	3.90	0.99	0.08	6.42	yes	G9VCN+1	0.55	1.41
HD15337	5179	4.39	0.70	0.06	9.10	no	K1V	0.58	<0.42
HD16270	4786	4.39	0.84	0.06	8.37	no	K3.5Vk:	<-0.32	<0.03
HD21019 ^b	5468	3.93	1.05	-0.45	6.20	no	G2V	0.22	1.39
HD27894	4952	4.39	0.78	0.20	9.42	yes	K2V	<-0.38	<0.22
HD35854	4928	4.46	0.54	-0.13	7.74	no	K2V	<-0.31	<-0.22
HD40105 ^b	5137	3.85	0.97	0.06	6.52	no	K1IV-V	<-0.12	1.40
HD44573	5071	4.48	0.80	-0.07	8.46	no	K2.5Vk:	0.75	<-0.01
HD63454	4840	4.30	0.81	0.06	9.37	yes	K3Vk:	<-0.32	<-0.03
HD93083	5105	4.43	0.94	0.09	8.33	yes	K2IV-V	<-0.14	<0.16
HD213042	4831	4.38	0.82	0.08	7.66	no	K5V	<-0.40	<0.06

^aValues taken from Simbad

^bEvolved stars

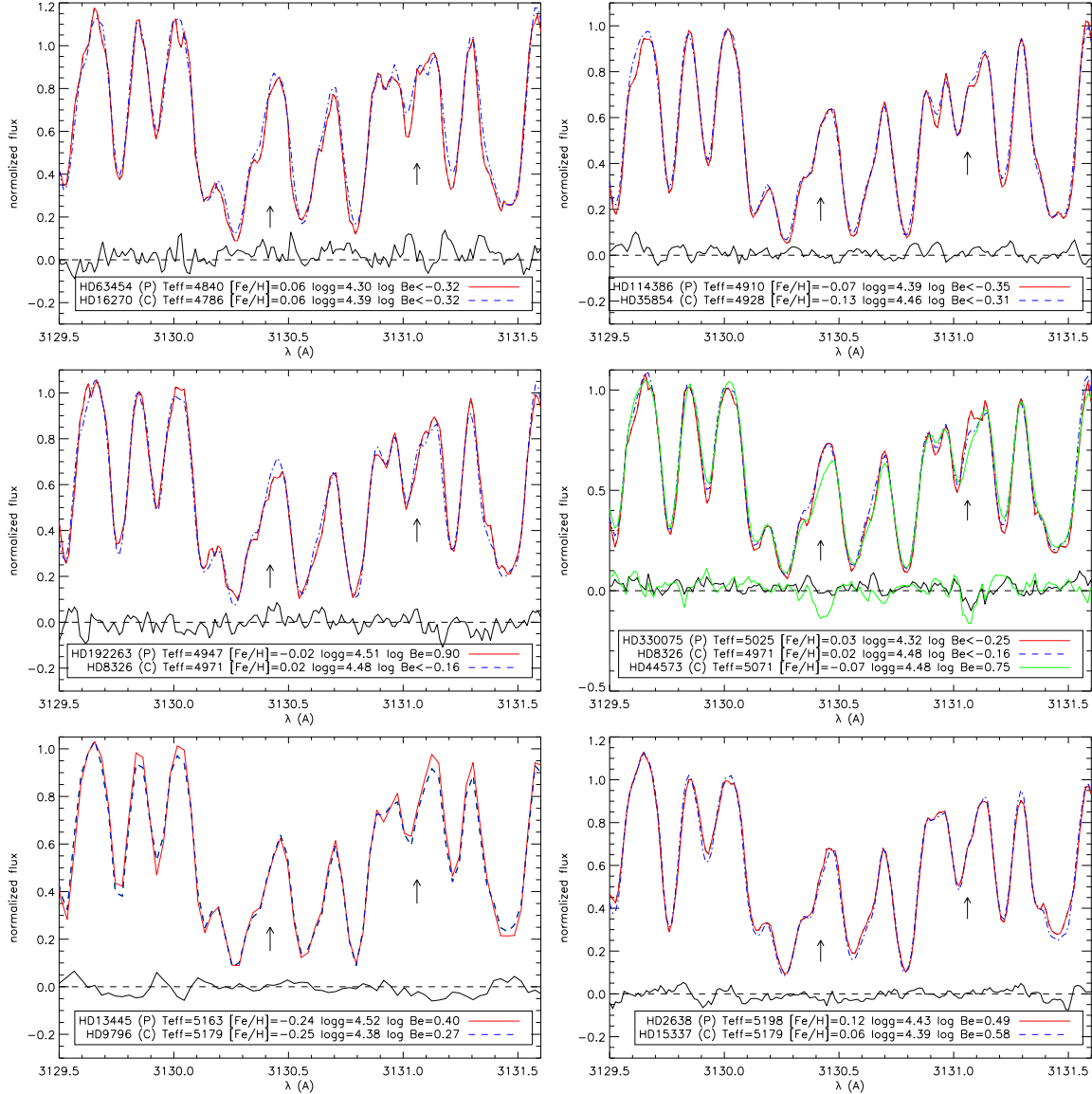


Fig. 3.— Observed spectra and difference in fluxes for six pairs of planet-host stars (red lines) and stars without detected planets (blue dashed lines). The position of Be lines are indicated by the arrows.

4.1. Is Be depleted in stars with planets?

We have seen in the previous section that absolute Be abundances determined with spectral synthesis are probably not reliable for cool stars, preventing a comparison between stars with and without detected planets. In order to search for differences in Be abundances between those stars

we proposed to compare directly their spectra in a previous paper (Delgado Mena et al. 2011). We selected pairs of stars with similar stellar parameters so if there were a difference between their spectra in the Be region it should be due to a difference in Be abundance. In that paper we presented two planet-host stars, HD 330075 and HD 13445, with an extra Be depletion when com-

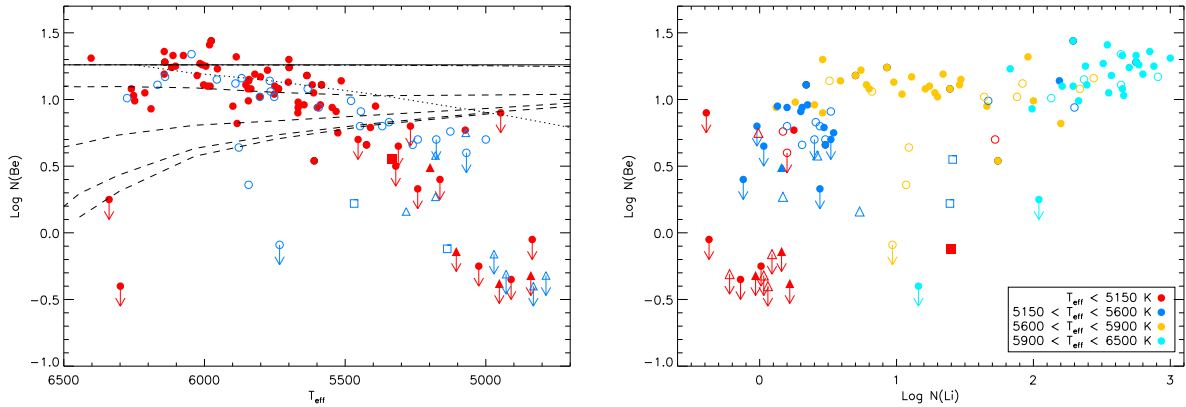


Fig. 4.— *Left panel:* Be abundances as a function of effective temperature for dwarf stars with and without detected planets from this work (red filled and blue open triangles, respectively) and dwarf stars with (red filled circles) and without planets (blue open circles) from previous studies (Santos et al. 2002, 2004a,c; Gálvez-Ortiz et al. 2011; Delgado Mena et al. 2011). The three evolved stars from this work are depicted with squares. The Sun is denoted by the usual symbol. The dashed lines represent 4 Be depletion models of Pinsonneault et al. (1990) (Case A) with different initial angular momentum for solar metallicity and an age of 1.7 Gyr. The solid line represents an assumed initial Be abundance of 1.26 Santos et al. (2004c). The dotted line represents the Be depletion isochrone for 4.6 Gyr taken from the models including mixing by internal waves of Montalbán & Schatzman (2000). *Right panel:* Be abundances as a function of Li abundances. Filled and open circles are stars with and without planets, respectively, from previous surveys. Filled and open triangles are stars with and without planets, respectively, from this work. Filled and open squares are evolved stars with and without detected planets, respectively, with measured Be abundance in this work. Colors denote different temperature ranges.

pared to analogous stars without detected planets, showing that the effect observed in Li abundances for solar-type stars with giant planets might also occur for Be in cooler stars.

In this work we present new spectra for 15 cool stars (see Table 2) with and without detected planets. Using these stars and others from previous works (Santos et al. 2004a,c; Gálvez-Ortiz et al. 2011; Delgado Mena et al. 2011) we made 13 new pairs of analogous stars with differences in T_{eff} , $\log g$ and $[\text{Fe}/\text{H}]$ lower than 50K, 0.15 dex and 0.10 dex respectively. We also note that $v \sin i$ values of these stars are very similar. Some examples of these couples are shown in Figure 3. We can see in these plots that stars with and without planets present similar Be features and the differences in flux between spectra are very low around Be features. In the previous paper we found three stars from the comparison sample with clearly higher Be abundance than the planet-host star HD 330075,

whose abundance is $\log \epsilon(\text{Be}) < -0.25$. Now we have two more stars with very similar parameters. HD 44573 has a higher Be abundance (see Table 2) and the difference in fluxes between both stars is around 5σ in the position of the two Be lines. However, HD 8326 has a spectrum very similar to HD 330075 and Be abundances are almost equal. Therefore, planet host stars and comparison stars can have similar Be abundances. We note, however, that our sample of cool stars is small and although unlikely, it might be possible that we are only observing the fraction of comparison stars with a strong Be depletion. A similar situation is seen for solar-type stars without detected planets, where 50% have high Li abundances while the other 50% do have its Li depleted like planet-hosts.

4.2. Be versus T_{eff}

In left panel of Figure 4 we plot the derived Be abundances as a function of effective temperature

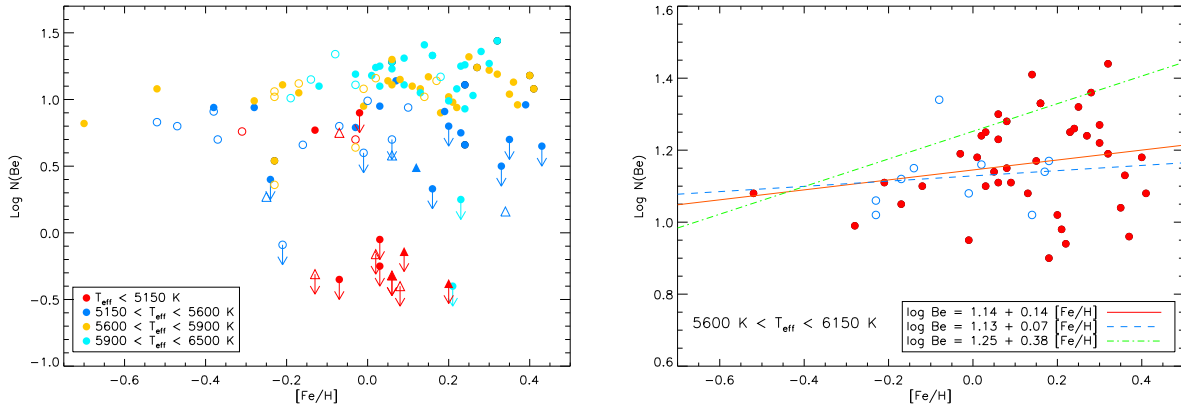


Fig. 5.— *Left panel*: Be abundances as a function of metallicity. Filled and open circles are dwarf stars with and without planets, respectively, from previous surveys. Filled and open triangles are dwarf stars with and without planets, respectively, from this work. Colors denote different temperature ranges. *Right panel*: Be abundances as a function of metallicity for dwarf stars with $5600 \text{ K} < T_{\text{eff}} < 6150 \text{ K}$ and detections of Be. We have overplotted two linear least square fittings for planet-host stars (red filled circles, red line) and stars without detected planets (blue open circles, blue dashed line).

for planet-host stars in our sample (see Table 2) together with previous samples. In this plot we have removed subgiants and giants (except the three analyzed in this work) to avoid evolutionary effects in the abundances. In this selection we took the spectral types of the stars from Gálvez-Ortiz et al. (2011). With this new sample of stars we have completed the coolest part of the plot and now we can see the behaviour of Be abundances in a wide range of effective temperatures.

As mentioned in previous papers, the Be abundances decrease from a maximum near $T_{\text{eff}} = 6100 \text{ K}$ towards higher and lower temperatures, in a similar way as Li abundances behave. In the high temperature domain, the steep decrease with increasing temperatures resembles the well known Be gap for F stars (e.g. Boesgaard & King 2002). The decrease of the Be content towards lower temperatures is smoother and may show evidence for continuous Be burning during the main sequence evolution of these stars.

When we move to the coolest stars, we observe a strong Be depletion regardless of the presence of planets. Hence, the planetary formation processes that affect Li depletion in solar analog stars (Israelian et al. 2009; Gonzalez et al. 2010) do not seem to take effect in the Be abundances.

On the other hand, we have found several stars with undetectable or very weak Be lines. The steep decrease of Be abundances for $T_{\text{eff}} < 5500 \text{ K}$ is in contradiction with models of Be depletion (Pinsonneault et al. 1990), which predict either constant or increasing Be abundances as T_{eff} decreases (see Figure 4). Even taking into account mixing by internal waves (Montalbán & Schatzman 2000), Be depletion is still lower than predicted. Be abundances have also been studied in clusters of different ages. Randich et al. (2007) found that stars in the 150 Myr old cluster NGC 2516 with $5000 < T_{\text{eff}} < 5500 \text{ K}$ have not depleted Be while Hyades stars (600 Myr) of the same T_{eff} present some Be depletion, something that cannot be explained by models with only convective mixing. García López et al. (1995) also found evidence of Be depletion for two cool Hyades members. Although uncertainties in Be abundances for the coolest stars are large and it might be some kind of systematic effect due to the Mn I $\lambda 3131.037 \text{ \AA}$ line, many of them seem to have their Be totally destroyed. Therefore, none of those models including convective mixing, rotation or gravitational waves seems to fit the observed Be abundances, at least at these cool temperatures. Other depletion mechanisms have been pro-

posed to explain Li destruction, such as tachocline diffusion (Brun et al. 1999; Piau et al. 2003) or episodic accretion of planetary material during the PMS (Baraffe & Chabrier 2010) though Be has not been analyzed. However, accretion of planetary material in the ZAMS (Théado et al. 2010; Théado & Vauclair 2011) can lead to an enhanced depletion of Li and Be, as well. These models can explain the difference in the Li abundances between stars with and without planets and might also explain the observed Be differences in a pair of cool planet-hosts when compared to several stars without detected planets (Delgado Mena et al. 2011). On the other hand the depletion produced by episodic accretion does not seem to be enough to explain the strong Be depletion observed in cool stars and the presence of planetary material would be necessary in all stars though many of them do not have detected planets.

4.3. Be versus Li

A beryllium versus lithium diagram can give us information about the depletion rates in main-sequence stars. In right panel of Figure 4 this relation is shown for all the stars in our sample. In general Be abundances increase with increasing Li abundances and stars with and without planets (filled and open symbols, respectively) behave in a similar way. If we take into account the effective temperatures we can divide the sample in four groups. The first one, with the hottest stars (light blue points), present both high Be and Li abundances except for two stars with T_{eff} around 6300K which fall in the Be-Li dip region, where the depletion of those elements is attributed to slow mixing and depends on age and temperature (Boesgaard & King 2002; Boesgaard et al. 2004a), though one of them, HD 120136 presents a normal Li abundance ($\log \epsilon(\text{Li}) = 2.04$). In the second group (orange points), with effective temperatures between 5600 and 5900 K, Be abundances remain high although Li abundances present different depletion rates. There are several objects with low Be abundances and solar temperatures (specially the comparison star HD 20766 $T_{\text{eff}} = 5733$ K, $\log \epsilon(\text{Be}) < -0.09$), which could form some kind of “Be-gap” where the depletion of Be may be related to different pre-main sequence ro-

tational histories (Santos et al. 2004c). In a recent work, Takeda et al. (2011) found four stars with solar temperatures and Be line undetectable. Those stars are also depleted in Li and have low $v \sin i$ values indicating that slow rotation can be the cause for that strong Be depletion.

In the third group (blue points), composed by stars with $5150\text{K} < T_{\text{eff}} < 5600\text{K}$, Be abundances begin to decrease and Li is severely depleted except for two objects, HD 11964A and HD 21019, with particularly high Li abundances considering its temperature. These two objects are evolved stars, therefore a possible explanation for the high Li content is that they have just left the main sequence, where they were hotter than they are now, but there has not been time for their Li and Be to become strongly depleted. Other possible explanations are a dredge up effect from a “buffer” below the former main sequence convective envelope (Deliyannis et al. 1990) or accretion of planetary metal-rich material, although recent models indicate that accretion of planetary material might destroy Li instead of producing an enhancement (Baraffe & Chabrier 2010; Théado et al. 2010). Finally, the coolest objects of our sample (red symbols) are depleted in both Be and Li, although some stars have preserved some Be. There are two objects with anomalous high Li content. HD 74576 seems to be a young star, something that probably justifies its high Li content (see discussion in Santos et al. 2004c) while HD 40105 is an evolved star that might have suffered some of the processes proposed for HD 11964A and HD 21019. We note that we have removed from the plots all the evolved stars from previous works. Only the three subgiants observed for this work are analyzed here but there are similar cases in the whole sample (see Santos et al. 2004c; Gálvez-Ortiz et al. 2011).

This figure confirms what found in Santos et al. (2004a,c); Gálvez-Ortiz et al. (2011), Be and Li burning seems to follow the same trend. Both elements increase their content as the temperature rises, although Li depletion begins at 5900 K while strong Be depletion starts below 5500 K. Stars with and without planets behave in a similar way.

4.4. Be versus [Fe/H]

In the left panel of Figure 5 we show Be abundances as a function of metallicity for different temperature ranges. We can see that the stars are equally distributed regardless of their temperature and for higher metallicities the dispersion in Be abundances increases, mainly due to objects with $5150 \text{ K} < T_{\text{eff}} < 5600 \text{ K}$. It is well known that Be abundances increase with metallicity for $[\text{Fe}/\text{H}] < -1$ with a steep slope near 1 (e.g. Rebolo et al. 1988; Boesgaard et al. 2009), but for higher metallicities this relation is not so well defined.

Boesgaard et al. (2004b) found a slope of 0.38 for stars with metallicity between -0.6 and 0.2, in agreement with Takeda et al. (2011) whose slope value is 0.49, although they take into account only solar analogs with $-0.3 < [\text{Fe}/\text{H}] < 0.3$. On the other hand, Boesgaard et al. (2009) argued that stars of one solar mass with solar metallicities (their most metallic star has $[\text{Fe}/\text{H}] = 0.11$) match the slope of 0.86 for metal-poor stars.

In the right panel of Figure 5 all the dwarf stars of our sample with $5600 \text{ K} < T_{\text{eff}} < 6150 \text{ K}$ are plotted. We have chosen this limit in temperature in order to remove most of the upper limits in Be abundances and those stars from the Li-Be dip. We have also removed stars from the solar Be-gap. We find a slope of 0.13 for planet-host stars and 0.07 for comparison sample stars. These values are lower than previously found by other authors but this could be possibly due to the lack of stars with $[\text{Fe}/\text{H}] < -0.2$ in our sample in comparison with the high number of metal-rich objects. It seems that stars with solar and supersolar metallicities do not follow the same trend as metal-poor stars, and Be has been produced at a lower rate as the Galaxy has evolved. However, we note that Be abundances present higher uncertainties in metal-rich stars that might be affecting these trends. If we have a look in the upper envelope, which might be more consistent with lower metallicity stars (around $[\text{Fe}/\text{H}] = -0.5$), we obtain a fit with a slope of 0.38, more consistent with previous results.

4.5. Be versus [O/H]

Beryllium is produced by spallation reactions between galactic cosmic rays (GCRs) and the CNO nuclei in the interstellar medium (see e.g. Tan et al. 2009, and references therein). There-

fore, oxygen abundances can provide us with complementary information about the galactic evolution of Be. We compile oxygen abundances from Ecuivillon et al. (2006) (see the final lists in Gálvez-Ortiz et al. 2011), derived with the OH bands in the near-UV since this region is closed to Be lines. We use the same temperature ranges than in previous section, $5600 \text{ K} < T_{\text{eff}} < 6150 \text{ K}$. Thus, none of the stars analyzed in this work are included in this plot because all of them are cooler than 5600 K. However, 6 planet-host stars from our previous work (Delgado Mena et al. 2011) are hotter and we have displayed them as green circles in Figure 6. Oxygen abundances for these stars have been obtained in the same way as Ecuivillon et al. (2006) and are presented in Table 3.

In the middle panel of Figure 6, Be abundances are plotted as a function of $[\text{O}/\text{H}]$. We can see that the slopes of planet hosts and stars without detected planets are slightly different, possibly due to the low number of comparison sample stars in this range. We have removed the star HD154857 since its O abundance is the lowest of this sample and its content in Be is considerable lower than other stars of similar oxygen abundance, hence it would increase the slope by 0.3. We make again a fit of the upper envelope for stars with planets to take into account the lack of stars with low $[\text{O}/\text{H}]$ in our plot. These trends might be influenced by the effect of T_{eff} in Be abundances. To remove this effect, we have made a new Be vs. $[\text{O}/\text{H}]$ plot (lower panel of Figure 6) with “corrected” Be abundances, calculated as $\log \epsilon(\text{Be}) - \log \epsilon(\text{Be}(T_{\text{eff}}))$, where $\log \epsilon(\text{Be}(T_{\text{eff}}))$ is obtained from a linear fit of Be as a function of temperature in the same T_{eff} range (upper panel of Figure 6). However, the slope is still the same for stars with planets. It seems that there remains a correlation between Be and O abundances, which may indicate that the sensitivity of Be to the T_{eff} is not affecting at all this correlation. On the other hand, the comparison sample is so small at this temperature range, that no strong

conclusion can be extracted from the different slopes obtained before and after the Be- T_{eff} linear correction.

Nevertheless, these slopes are considerable lower than previously found for metal-poor stars,

TABLE 3
 OXYGEN ABUNDANCES FOR STARS WITH $T_{\text{eff}} > 5400$ K FROM DELGADO MENA ET AL. (2011).

Star	[O/H] ₁	[O/H] ₂	[O/H] ₃	[O/H] ₄	[O/H] _{final}	log $\epsilon(\text{Be})$
HD2039	0.17	0.12	0.17	0.29	0.18	1.44
HD4203	0.08	0.01	0.22	0.20	0.13	1.18
HD73526	-	-	0.20	0.25	0.22	1.24
HD76700	0.16	0.16	0.28	0.35	0.24	1.08
HD154857	-0.23	-0.20	-0.18	-0.18	-0.20	0.54
HD208847	0.13	0.08	0.05	0.10	0.09	1.28
HD216770	-0.01	0.04	0.06	0.06	0.04	0.66

even the slope of the upper envelope in the middle panel. Boesgaard et al. (1999) obtained a slope of 1.45, using stars with $-3 < [\text{Fe}/\text{H}] < 0.05$, while Tan et al. (2009) reported a slope of 1.49, for stars with $-2.3 < [\text{Fe}/\text{H}] < -0.6$. Therefore, the slope for metal-rich stars is much flatter than for metal-poor stars as it seems to happen for Be versus $[\text{Fe}/\text{H}]$. A slope like this would not be in agreement with models of Be production that predict quadratic or linear relations (see e.g. Tan et al. 2009, and references therein). We note again that oxygen abundances present a high dispersion in metal-rich stars and even at low metallicities, the use of different O indicators change this trend.

5. Conclusions

We present new high-resolution UVES/VLT near-UV spectra of 15 stars with and without planets in order to find possible differences in Be abundances between them and confirm our previous results that suggested a greater depletion of Be in planet-host stars when compared with stars without detected planets. Be needs higher temperatures than Li to be destroyed so we have to search for these differences in cooler stars, which have deeper convective envelopes and are able to carry the material towards Be-burning layers. We have made new couples of analog stars with and without planets with the purpose of comparing directly their spectra to see possible differences in Be abundances. Although in a previous work we found a pair of planet-host stars with their Be severely depleted, now we have not observed important differences in Be abundances between both groups of stars. Thus, the effect caused by

protoplanetary disks and rotational history on extra Li depletion in solar-type stars with planets is not taking effect in Be abundances, apparently.

Furthermore, Be abundances in cool stars ($T_{\text{eff}} < 5200$ K) are much lower than predicted by the models. We have analyzed for the first time a considerable number of cool objects and found a strong destruction of Be in most of the stars. Although we cannot provide absolute abundances we can give upper values for Be. This gives a steep drop of Be abundances as T_{eff} diminishes in contradiction with current models of Be depletion.

Finally, the slopes of Be abundances as a function of $[\text{Fe}/\text{H}]$ and $[\text{O}/\text{H}]$ are considerably lower than found for metal-poor stars, indicating that the production rate of Be may have diminished with the evolution of the Galaxy.

E.D.M, J.I.G.H. and G.I. would like to thank financial

support from the Spanish Ministry project MICINN AYA2008-04874.

J.I.G.H. acknowledges financial support from the Spanish Ministry of

Science and Innovation (MICINN) under the 2009 Juan de la Cierva

Programme.

N.C.S. would like to thank the support by the European Research Council/European Community under the FP7 through a

Starting Grant, as well from Fundação para a Ciência e a Tecnologia (FCT), Portugal, through a Ciência2007 contract funded by FCT/MCTES (Portugal) and POPH/FSE (EC), and in the form of grant reference PTDC/CTE-AST/098528/2008 from FCT/MCTES.

This research has made use of the SIMBAD database operated at CDS, Strasbourg, France.

This work has also made use of the IRAF facility, and the Encyclopaedia of extrasolar planets.

REFERENCES

- Baraffe, I., & Chabrier, G. 2010, *A&A*, 521, A44
- Baumann, P., Ramírez, I., Meléndez, J., Asplund, M., & Lind, K. 2010, *A&A*, 519, A87
- Boesgaard, A. M., Armengaud, E., King, J. R., Deliyannis, C. P. & Stephens, A. 2004, *ApJ*, 613, 1202
- Boesgaard, A. M., Deliyannis, C. P., King, J. R., Ryan, S. G., Vogt, S. S. & Beers, T. C. 1999 *AJ*, 117, 1549
- Boesgaard, A. M., McGrath, E. J., Lambert, D. L. & Cunha, K. 2004, *ApJ*, 606, 306
- Boesgaard, A. M. & Hollek, J. K. 2009, *AJ*, 691, 1412
- Boesgaard, A. M. & King, J. R. 2002, *ApJ*, 565, 587
- Bouvier, J. 2008, *A&A*, 489, 53
- Brun, A. S., Turck-Chièze, S., & Zahn, J. P. 1999, *ApJ*, 525, 1032
- Castro, M., Vauclair, S., Richard, O. & Santos, N. C. 2009, *A&A*, 494, 663
- Chen, Y. Q., & Zhao, G. 2006, *AJ*, 131, 1816
- Delgado Mena, E., Israelian, G., González Hernández, J. I., Santos, N. C., & Rebolo, R. 2011, *ApJ*, 728, 148
- Deliyannis, C. P., Cunha, K., King, J. R. & Boesgaard, A. M. 2000, *AJ*, 119, 2437
- Deliyannis, C. P., Demarque, P. & Kawaler, S. 1990, *ApJS*, 73, 21
- Ecuivillon, A., Israelian, G., Santos, N. C., Shchukina, N. G., Mayor, M., & Rebolo, R. 2006, *A&A*, 445, 633
- Eggenberger, P., Maeder, A. & Meynet, G. 2010, *A&A*, 519, L2

- Gálvez-Ortiz, M.C., Delgado Mena, E., González Hernández, J.I., Israelian, G., Santos, N. C., & Rebolo, R. 2011, *A&A*, *accepted*
- García López, R. J. & Pérez de Taoro, M. R. 1998, *A&A*, 334, 599
- García López, R. J., Rebolo, R. & Pérez de Taoro, M. R. 1995, *A&A*, 302, 184
- Gilli, G., Israelian, G., Ecuivillon, A., Santos, N. C., & Mayor, M. 2006, *A&A*, 449, 723
- Gonzalez, G. 1998, *A&A*, 334, 221
- Gonzalez, G. 2008, *MNRAS*, 386, 928
- Gonzalez, G., Carlson, M. K., & Tobin, R. W. 2010, *MNRAS*, 403, 1368
- Gonzalez, G., Laws, C., Tyagi, S. & Reddy, B. E. 2001, *AJ*, 121, 432
- Fischer, D.A. & Valenti, J. 2005, *AJ*, 622, 1102
- Israelian, G., Santos, N. C., Mayor, M., & Rebolo, R. 2004, *A&A*, 414, 601
- Israelian, G., et al. 2009, *Nature*, 462, 189
- Kurucz, R. L. 1993, *ATLAS9 Stellar Atmospheres Programs and 2 kms⁻¹ Grid (CD-ROM, Smithsonian Astrophysical Observatory, Cambridge)*
- Montalbán, J. & Schatzman, E. 2000, *A&A*, 354, 943
- Neves, V., Santos, N. C., Sousa, S. G., Correia, A. C. M. & Israelian, G. 2009, *A&A*, 497, 563
- Pasquini, L., Biazzo, K., Bonifacio, P., Randich, S. & Bedin, L. R. 2008, *A&A*, 489, 677
- Piau, L., Randich, S., & Palla, F. 2003, *A&A*, 408, 1037
- Pinsonneault, M. H., Kawaler, S. D. & Demarque, P. 1990, *ApJS*, 74, 501
- Primas, F., Duncan, D. K., Pinsonneault, M. H., Deliyannis, C. P., & Thorburn, J. A. 1997, *ApJ*, 480, 784
- Randich, S., Primas, F., Pasquini, L., Sestito, P., & Pallavicini, R. 2007, *A&A*, 469, 163
- Rebolo, R., Abia, C., Beckman, J. E., & Molaro, P. 1988, *A&A*, 193, 193
- Santos, N. C., García López, R. J., Israelian, G., Mayor, M., Rebolo, R., García-Gil, A., Pérez de Taoro, M. R., & Randich, S. 2002, *A&A*, 386, 1028
- Santos, N. C., Israelian, G., García López, R. J., Mayor, M., Rebolo, R., Randich, S., Ecuivillon, A., & Domínguez Cerdeña, C. 2004a, *A&A*, 427, 1085
- Santos, N. C., Israelian, G. & Mayor, M. 2000, *A&A*, 363, 228
- Santos, N. C., Israelian, G. & Mayor, M. 2001, *A&A*, 373, 1019
- Santos, N. C., Israelian, G., & Mayor, M. 2004b, *A&A*, 415, 1153
- Santos, N. C., Israelian, G., Mayor, M., Bento, J. P., Almeida, P. C., Sousa, S. G., & Ecuivillon, A., 2005, *A&A*, 437, 1127
- Santos, N. C., Israelian, G., Randich, S., García López, R. J., & Rebolo, R. 2004c, *A&A*, 425, 1013

Sestito, P. & Randich, S. 2005,
A&A, 442, 615

Sousa, S. G., Fernandes, J., Israelian, G., & Santos, N. C. 2010,
A&A, 512, L5

Sousa, S.G., Santos, N.C., Mayor, M., Udry, S.,
Casagrande, L., Israelian, G., Pepe, F., Queloz,
D. & Monteiro, F.G. 2008,
A&A, 487, 373

Smiljanic, R., Randich, S., & Pasquini, L. 2011,
arXiv:1108.0776

Snedden, C. 1973 Ph.D Thesis, University of Texas.

Stephens, A., Boesgaard, A. M., King, J. R., &
Deliyannis, C. P. 1997,
ApJ, 491, 339

Tan, K. F., Shi, J. R.,
& Zhao, G. 2009, MNRAS, 392, 205

Takeda, Y., Kawanomoto, S., Honda, S., Ando,
H., & Sakurai, T. 2007,
A&A, 468, 663

Takeda, Y., Tajitsu, A., Honda, S., Kawanomoto,
S., Ando, H., & Sakurai, T. 2011,
arXiv:1103.5275

Théado, S., Bohun, E., & Vauclair, S. 2010,
IAU Symposium, 268, 427

Théado, S., & Vauclair, S. 2011, arXiv:1109.4238

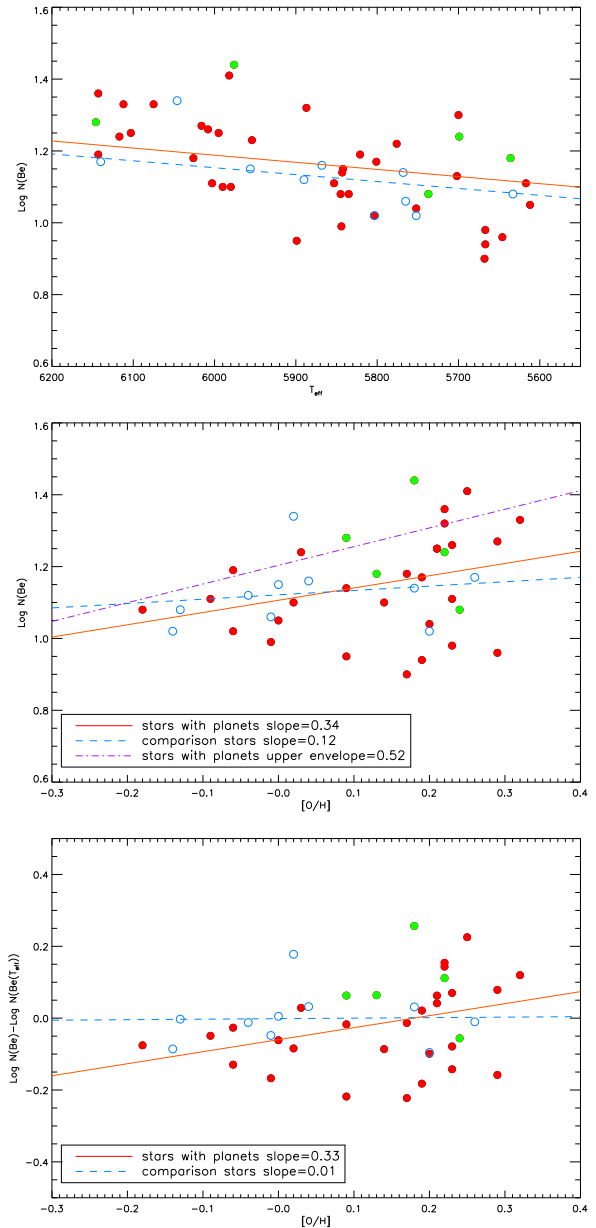


Fig. 6.— *Upper panel:* Be abundances as a function of temperature for dwarf stars with effective temperature between 5600 K and 6150 K with (red filled circles) and without planets (blue open circles). Green circles are stars with planets with oxygen abundances measured in this work. *Middle panel:* Be abundances as a function of $[\text{O}/\text{H}]$ using O abundances from OH (Ecuivillon et al. 2006) lines for stars with effective temperature between 5400 K and 6300K. Symbols like in top panel. *Lower panel:* Be abundances corrected of temperature effect for the same stars than middle panel.

This 2-column preprint was prepared with the AAS L^AT_EX macros v5.2.